

# OVOD-Agent: A Markov-Bandit Framework for Proactive Visual Reasoning and Self-Evolving Detection

Chujie Wang\* Jianyu Lu\* Zhiyuan Luo Xi Chen† Chu He†  
 Wuhan University  
 chujie@whu.edu.cn

## Abstract

*Open-Vocabulary Object Detection (OVOD) aims to enable detectors to generalize across categories by leveraging semantic information. Although existing methods are pre-trained on large vision-language datasets, their inference is still limited to fixed category names, creating a gap between multimodal training and unimodal inference. Previous work has shown that improving textual representation can significantly enhance OVOD performance, indicating that the textual space is still underexplored. To this end, we propose OVOD-Agent, which transforms passive category matching into proactive visual reasoning and self-evolving detection. Inspired by the Chain-of-Thought (CoT) paradigm, OVOD-Agent extends the textual optimization process into an interpretable Visual-CoT with explicit actions. OVOD’s lightweight nature makes LLM-based management unsuitable; instead, we model visual context transitions as a Weakly Markovian Decision Process (w-MDP) over eight state spaces, which naturally represents the agent’s state, memory, and interaction dynamics. A Bandit module generates exploration signals under limited supervision, helping the agent focus on uncertain regions and adapt its detection policy. We further integrate Markov transition matrices with Bandit trajectories for self-supervised Reward Model (RM) optimization, forming a closed loop from Bandit exploration to RM learning. Experiments on COCO and LVIS show that OVOD-Agent provides consistent improvements across OVOD backbones, particularly on rare categories, confirming the effectiveness of the proposed framework.*

## 1. Introduction

Open-Vocabulary Object Detection (OVOD) aims to extend object detectors to arbitrary concepts by exploiting the semantic priors learned from large-scale vision–language pre-training [12, 21, 32, 43, 44]. With improved region–text alignment and large-vocabulary modeling [4, 25, 38–40], recent methods have substantially enhanced open-set recog-

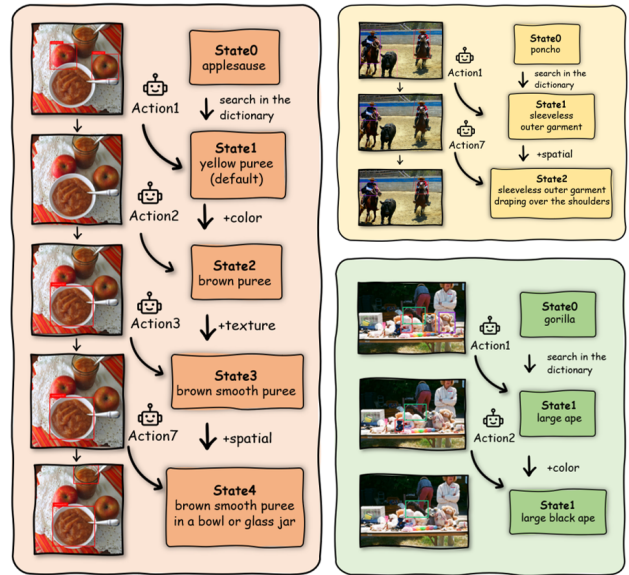


Figure 1. We illustrate the state-transition behavior of OVOD-Agent as it iteratively updates its category hypothesis. Starting from an initial dictionary lookup, the agent applies attribute-aware actions that adjust color, texture, and spatial cues to produce a more accurate and grounded state description. The number of required actions varies across images, from single-step updates to multi-step reasoning.

niton. However, although these models are trained with multimodal supervision, their inference still depends on a fixed set of category names. This turns detection into a simple matching routine and creates a clear mismatch between multimodal training and unimodal inference. Consequently, existing methods struggle to reason under visual ambiguity, adapt to unfamiliar contexts, and detect rare or fine-grained categories.

A growing body of work has shown that the textual space has a much greater impact on OVOD performance than previously assumed. Techniques such as prompt learning [8], prompt diversification [11], attribute-based descriptions [31], and automatic class-name optimization [29] con-

sistently reshape the textual embedding space and lead to marked improvements across OVOD benchmarks, suggesting that this space remains far from saturated [2]. To enrich fine-grained semantics, recent studies introduce LLM-generated priors to expand the textual domain [16, 26]. Yet these approaches remain essentially static: a single adjustment to the descriptor cannot capture the evolving relationships among regions, contexts, and attributes during detection. What is still lacking is a context-dependent, iterative mechanism that can continuously refine textual representations throughout inference.

The step-by-step reasoning paradigm of CoT [36], together with advances in interactive vision–language agents [9, 34, 41], has enabled multi-step visual operations in multimodal systems. Frameworks such as Visual-CoT [22, 35] suggest that visual cues can be aligned with textual semantics through progressive reasoning. In OVOD, CoT-PL [5] further shows that incorporating such reasoning during training can improve the quality of pseudo labels. However, these approaches inherit the agent-style design that places an LLM at the center of the decision process [5, 16], which imposes substantial computational and memory overhead during inference. Some even rely on multiple rounds of human feedback to guide the reasoning procedure [18]. Such designs run counter to the core strengths of object detection—speed, scalability, and ease of deployment—and ultimately make the pipeline unnecessarily heavy for the OVOD setting.

To address these limitations, we introduce OVOD-Agent, a lightweight and LLM-free framework that transforms OVOD from passive category matching into proactive visual reasoning and self-evolving detection. We model the evolution of visual and semantic cues as a Weakly Markovian Decision Process (w-MDP) defined over eight compact visual states, which provides a structured view of state transitions and memory and serves as the foundation for our agent formulation. A Bandit-based exploration module identifies uncertain or semantically ambiguous regions, generating informative trajectories for adaptive refinement. We further couple Markov transition statistics with these trajectories to train a self-supervised Reward Model (RM), forming a closed loop that enables continuous policy improvement under weak supervision. Experiments on COCO and LVIS show that OVOD-Agent consistently enhances existing OVOD backbones while adding only limited deployment overhead (<100 MB disk, <20 MB memory) and <100 ms latency cost, demonstrating its practicality for real-world deployment. In summary, the main contributions are as follows:

- We introduce OVOD-Agent, which models visual context transitions using an eight-state weak MDP and converts static prompt matching into an interpretable multi-step Visual-CoT reasoning process with explicit actions, in-

teraction, and memory.

- We propose a Bandit-based exploration strategy for collecting trajectories under uncertain visual states and combine global Markov transition statistics with offline trajectories to train a self-supervised Reward Model, forming a closed-loop mechanism for agent self-evolution.
- Our framework introduces no large-model dependencies, incurs minimal inference overhead, preserves the deployment efficiency of existing detectors, and remains compatible with a wide range of OVOD backbones.

## 2. Related Work

**LLM-Based Textual Optimization** Large language models (LLMs) have recently been adopted to enhance textual representations in vision–language tasks [20, 24, 30, 45]. In OVOD, LLMs are increasingly used to enrich category descriptors, generate fine-grained attributes, or provide contextual priors [16, 26]. Such approaches substantially expand the semantic coverage of textual embeddings and often improve zero-shot recognition performance. However, LLM-centric frameworks typically introduce heavy computational and storage overhead due to their large parameter scales, and many require multi-round human feedback or instruction tuning [18]. These characteristics contradict the long-standing strengths of object detectors—efficiency, scalability, and deployability. Our work differs by avoiding LLM dependence entirely and focusing on lightweight, inference-time refinement.

**Lightweight Textual Enhancement and Discrete Alignment** Retrieval-augmented generation (RAG) [10] offers a simple and effective way to enrich textual descriptions by retrieving semantically relevant information from large corpora. In OVOD, however, generating high-quality retrieval vectors from limited visual evidence remains a significant challenge. RALF [17] addresses this issue by training an OVOD-specific retrieval module and further augments textual prompts with generative completion [15], effectively mitigating the lack of textual diversity. Yet these improvements remain fundamentally single-step and cannot support iterative, state-dependent reasoning, making it difficult to emulate the multi-step reasoning patterns observed in LLM-style Chain-of-Thought [9, 34, 41]. Several alignment-based approaches [33, 42] demonstrate that region–text matching exhibits strong discreteness, where small perturbations in the textual space can lead to substantial shifts in detection behavior. This observation provides an important insight: coarse-to-fine, discrete transitions in the semantic space can act as a structured alternative to the continuous reasoning typically associated with LLM-based CoT. Markov-based formulations [7, 37] further support this viewpoint by showing that discrete semantic transitions can approximate complex reasoning procedures typ-

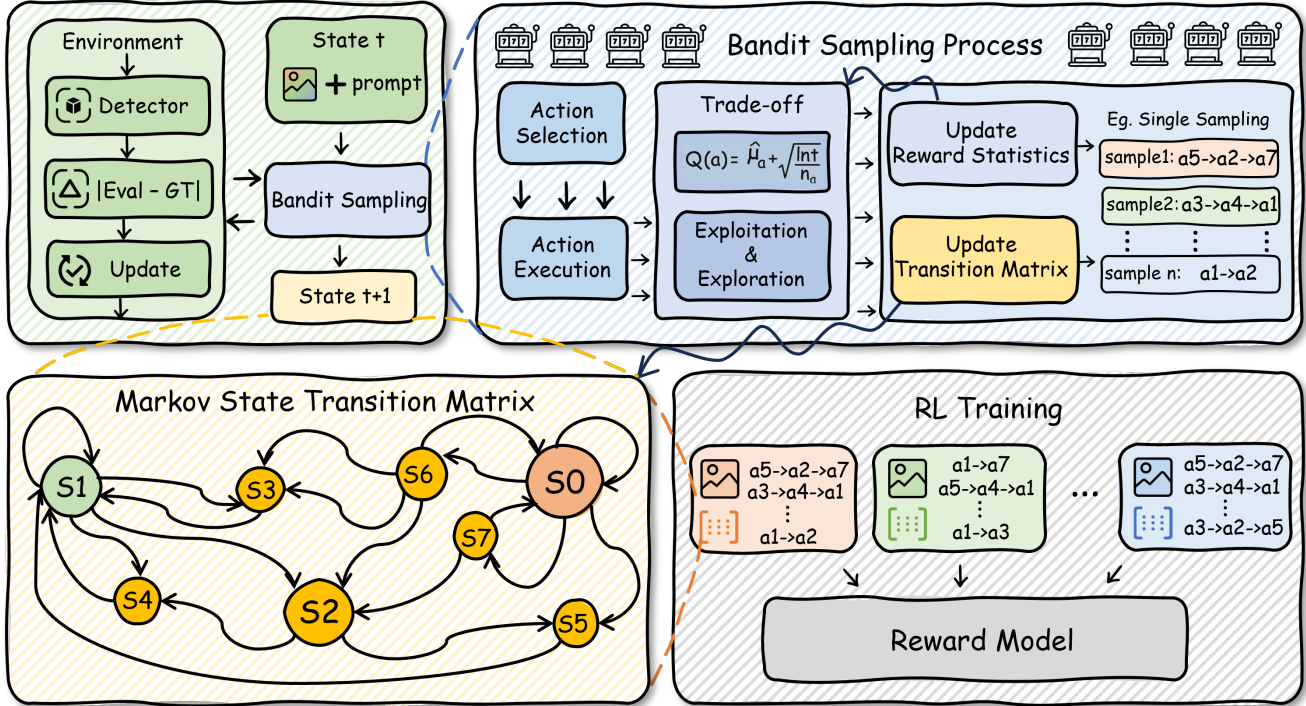


Figure 2. OVOD-Agent operates through a self-evolving visual reasoning pipeline. (a) The environment updates the visual state by applying detector feedback and the current prompt-conditioned context. (b) A UCB-based Bandit module selects and executes visual actions, collecting rewards and empirical transitions from sampled trajectories. (c) The collected trajectories are joined into an image-specific Markov transition matrix that models how weak Markov units evolve under different visual operations and serves as a structured prior for learning. (d) A lightweight Reward-Policy Model (RM) is trained on these trajectories and transition priors, distilling both transition behavior and weak reward signals. During inference, the RM replaces Bandit exploration and directly guides the agent’s step-by-step refinement process without relying on LLMs.

ically attributed to LLMs. Our work builds on this line of thought by treating OVOD inference as a structured decision process. Instead of continuous textual manipulation or heuristic prompt engineering, we adopt a Weakly Markovian Decision Process (w-MDP) to model discrete visual-semantic transitions within a compact state space.

### Sequential Decision Making and Bandit Exploration

Reinforcement learning (RL) has been widely explored for sequential decision-making in vision systems [3, 6, 14, 28]. However, full RL pipelines are impractical in OVOD due to limited supervision and the high cost of rollout-based training. Lightweight exploration methods such as multi-armed and contextual Bandits [1, 19] offer a more suitable alternative, providing uncertainty-driven sampling without the overhead of policy learning. In our approach, Bandit exploration identifies uncertain or semantically ambiguous states and supplies informative transitions for downstream reward estimation. Combined with Markov transition statistics, this yields a compact and efficient Markov-Bandit reinforcement mechanism tailored to OVOD.

## 3. Method

In this section, we introduce OVOD-Agent, a lightweight self-evolving visual agent for open-vocabulary object detection, as illustrated in Fig. 2. We first present the problem formulation and the agent foundation in Sec. 3.1-3.2, followed by the data sampling procedure in Sec. 3.3, and finally the training strategy and full evolution loop in Sec. 3.4-3.5.

### 3.1. Problem Setup and Notation

**Core Idea.** Traditional OVOD systems rely on static one-shot matching between text and visual regions, lacking the ability to jointly reason about and adjust the matching space. We aim to establish a proactive visual reasoning paradigm, where the detector actively executes a sequence of explicit visual operations under the current visual state to iteratively refine its textual representation, forming an interpretable *Visual Chain-of-Thought* (Visual-CoT).

**Formulation.** Given an image  $x$  and an open-vocabulary text prompt  $T$ , a detector  $D$  outputs region proposals and

category scores:

$$p = D(x, T). \quad (1)$$

To introduce reasoning ability, we define a context  $c_t = (x_t, T_t)$  and execute an explicit visual action  $a_t \in \mathcal{A}$  at each step:

$$c_{t+1} = f(c_t, a_t), \quad t = 0, 1, \dots \quad (2)$$

where  $f(\cdot)$  denotes a deterministic or stochastic transformation over the visual context, such as color cue extraction, ROI-based context adjustment, or texture analysis. This context-driven interaction process defines our agent prototype, **OVOD-Agent**.

**Action Space.** We define seven interpretable primitive visual operations that constitute the agent’s visual reasoning language:

Table 1. Seven interpretable visual operators forming the agent’s reasoning language.

| ID    | Action     | Explanation                                |
|-------|------------|--|
| $a_1$ | Dictionary | Alias/backoff; synonyms and hypernyms      |
| $a_2$ | Color      | HSV / cluster-based visual color cues      |
| $a_3$ | Texture    | Texture analysis (LBP/GLCM)                |
| $a_4$ | Background | FG/BG context analysis; ROI adjustment     |
| $a_5$ | Geometry   | Geometric properties (scale, aspect ratio) |
| $a_6$ | Lighting   | Illumination/shadow analysis (HSV-V)       |
| $a_7$ | Spatial    | Spatial relation analysis (position, IoU)  |

Each operator represents one step of visual reasoning, providing a lightweight and interpretable cue within the agent’s visual context.

### 3.2. Weak Markovian Modeling

**Weak Markov Process (w-MDP).** A Markov Decision Process (MDP) models decision-making based solely on the current state, naturally fitting agent design by describing the evolution of state, action, and memory. In conventional Markov decision settings, the state  $s_t$  and action  $a_t$  are strictly separated, with the transition dynamics defined as:

$$P(s_{t+1} | s_t, a_t). \quad (3)$$

However, in proactive visual reasoning, this separation becomes unnecessary. Visual actions—based on color, texture, geometric, lighting, or spatial cues—directly update the image-text context and inherently determine the next state. Moreover, the contextual evolution of these weak units is further recorded during Bandit-driven sampling in Sec. 3.3. We therefore propose a **Weakly Markovian Decision Process (w-MDP)**, where state and action are unified into a single weak Markov unit:

$$z_t = g(c_t, a_t) \in \mathcal{Z}, \quad (4)$$

with  $c_t = (x_t, T_t)$  denoting the current context and  $a_t$  the visual operation. This unified representation captures both the contextual semantics and the applied operation, reducing the agent’s context burden and forming a compact weak Markov unit on which the transition is defined.

The transition is defined as:

$$P(z_{t+1} | z_t), \quad (5)$$

under a short-term memory assumption:

$$P(z_{t+1} | z_t, z_{t-1}, \dots) \approx P(z_{t+1} | z_t). \quad (6)$$

This unified formulation preserves interpretability and avoids enumerating explicit state-action pairs, enabling lightweight transition updates. Thus, w-MDP provides a coherent framework for subsequent Bandit exploration and reinforcement distillation—each weak unit is both the result of reasoning and the starting point for the next step.

**Base Markov Field Initialization.** Under limited supervision, we initialize a base weak-Markov structure on the weak unit  $z_0$ , ensuring that both rewards and transitions are properly regularized to avoid early-stage random exploration.

**Reward Baseline (GT-seeded).** A weak reward is defined from the mismatch between predicted and ground-truth bounding boxes:

$$r_t^{GT} = 1 - \text{IoU}(b_t^{pred}, b_t^{GT}), \quad (7)$$

which serves as a quality baseline for each  $z_t$ . A higher  $r_t^{GT}$  indicates greater uncertainty, implying that the current state requires further refinement.

**Transition Prior (Dirichlet).** When data are scarce, each weak unit is assigned an outgoing prior distribution:

$$\hat{P}(\cdot | z_t) \leftarrow \text{Dirichlet}(\mathbf{n}_{z_t}), \quad (8)$$

where  $\mathbf{n}_{z_t}$  denotes pseudo-counts of candidate actions, typically initialized as a uniform vector. This prior guarantees probability normalization and structural feasibility for subsequent updates.

These two components jointly form the **Base Markov Field**: the GT-based reward provides weak supervision at the reward level, while the Dirichlet prior imposes structural regularization at the transition level. Together, they stabilize Bandit-driven exploration and guide early reasoning trajectories toward meaningful regions of the state space.

### 3.3. Bandit-Based Exploration Strategy

**Exploration Motivation.** Instead of pursuing a deterministic optimal solution per image, OVOD-Agent aims to sample diverse and high-quality reasoning trajectories for training. Random exploration is inefficient, while greedy selection easily converges to local optima. We adopt a **UCB-based contextual Bandit** strategy to balance exploration and exploitation.

**Action Selection.** For each context  $c_t$ , the local mean reward and visit count are denoted as  $\hat{\mu}_t(a | c_t)$  and  $n_t(a | c_t)$ . The decision rule is:

$$Q_t(a) = \hat{\mu}_t(a | c_t) + \lambda \sqrt{\frac{\ln t}{1 + n_t(a | c_t)}}, \quad (9)$$

$$a_{t+1} = \arg \max_a Q_t(a), \quad (10)$$

where  $\lambda$  controls exploration strength. After executing  $a_{t+1}$ , the transition distribution is updated via a Dirichlet prior:

$$\hat{P}(\cdot | z_t) \leftarrow \text{Dirichlet}(\mathbf{n}_{z_t} + \mathbf{e}_{z_{t+1}}). \quad (11)$$

This update maintains Markov consistency and stabilizes exploration.

**Stopping Criteria.** Each trajectory stops when one of the following holds:

- State stabilization:  $\|c_{t+1} - c_t\| < \delta_s$ ;
- Reward convergence:  $|r_{t+1} - r_t| < \delta_r$ ;
- Step limit:  $t \geq H_{\max} = 7$ .

At the image level, sampling terminates when:

- Mean reward increment  $\Delta \bar{r} < \epsilon_r$ ;
- Transition matrix convergence  $\|\hat{P}_{k+1} - \hat{P}_k\|_F < \epsilon_P$ ;
- Maximum episode limit  $E_{\max} = 50$ .

Default thresholds are set to:  $\delta_s = 0.02$ ,  $\delta_r = 10^{-3}$ ,  $\epsilon_r = \epsilon_P = 10^{-3}$ .

### 3.4. Reinforcement via Markov-Bandit Feedback

**Trajectory Dataset.** For each image  $x_i$ , the Bandit procedure in Sec. 3.3 generates multiple weak Markov trajectories,

$$\mathcal{T}_i = \{(z_t^{(m)}, z_{t+1}^{(m)}, r_t^{(m)})\}_{t,m}, \quad (12)$$

together with an empirical transition prior  $\hat{P}_i(\cdot | z)$  estimated from Dirichlet updates. The offline trajectory dataset is then

$$\mathcal{D} = \{(\mathcal{T}_i, \hat{P}_i)\}_{i=1}^N. \quad (13)$$

**Reward-Policy Model (RM).** Given the offline dataset  $\mathcal{D}$ , the RM is designed as a lightweight dual-head network comprising:

- **Policy head**  $\pi_\theta(\cdot | z_t)$ , modeling local transition continuity;
- **Reward head**  $\hat{r}_\theta(z_t)$ , predicting the expected weak reward.

**Joint Objective.** The RM is trained to recover the transition behavior and reward patterns encoded in the sampled trajectories  $\mathcal{T}_i$  and their corresponding transition priors  $\hat{P}_i$ .

---

### Algorithm 1: OVOD-Agent: Markovian Evolution

---

**Input** : Image  $x$ , Prompt  $T$ , Detector  $D$

**Params**: Actions  $\mathcal{A} = \{a_1, \dots, a_7\}$ ; RM  $(\pi_\theta, \hat{r}_\theta)$ ;

UCB coefficient  $\lambda$ ; thresholds

$\delta_s, \delta_r, \epsilon_r, \epsilon_P$ ; limits  $H_{\max}, E_{\max}$

**Output**: Reasoning trajectories and final detections

```

1 Initialize:  $c_0 \leftarrow (x, T)$ ,  $a_0 \leftarrow \text{Dictionary}$ ;
  buffer  $\mathcal{D} \leftarrow \emptyset$ 
2 for  $episode = 1$  to  $E_{\max}$  do
3    $t \leftarrow 0$ ;  $\mathcal{T} \leftarrow \emptyset$ ; initialize Dirichlet counts
    $\{\mathbf{n}_z\}$ 
4   while not TrajStop( $c_t, r_{t-1}, t$ ) do
5      $z_t \leftarrow g(c_t, a_t)$  // weak Markov unit
6      $a_{t+1} \leftarrow \arg \max_{a \in \mathcal{A}} \left[ \hat{\mu}(a | c_t) + \lambda \sqrt{\frac{\ln \max(2, t)}{1 + n(a | c_t)}} \right]$ 
7      $c_{t+1} \leftarrow f(c_t, a_{t+1})$ 
8      $(\text{boxes}_{t+1}, \text{scores}_{t+1}) \leftarrow D(c_{t+1})$ 
9      $r_t \leftarrow \text{UncertaintyReduction}(\text{scores}_t, \text{scores}_{t+1})$ 
10    update  $\mathbf{n}_{z_t}$  with the observed successor  $z_{t+1}$ 
11     $\mathcal{T} \leftarrow \mathcal{T} \cup \{(z_t, z_{t+1}, r_t)\}$ 
12     $t \leftarrow t + 1$ 
13  compute  $\hat{P}(\cdot | z)$  from Dirichlet
14   $\mathcal{D} \leftarrow \mathcal{D} \cup \{(\mathcal{T}, \hat{P})\}$ 
15  if ImageStop( $\mathcal{D}, \epsilon_r, \epsilon_P$ ) then
16    break

17 Offline Training: minimize  $\mathcal{L}_{\text{RM}}$  on  $\mathcal{D}$  to update  $\theta$ 
18 Inference: replace UCB with RM decision rules
   (policy-, reward-, or hybrid-driven) to select  $z_{t+1}$ 

```

---

Its learning objective integrates three components:

$$\begin{aligned} \mathcal{L}_{\text{RM}} = & \underbrace{\mathbb{E}_{(z_t, z_{t+1}) \sim \mathcal{D}} [-w_t \log \pi_\theta(z_{t+1} | z_t)]}_{\text{trajectory distillation}} \\ & + \beta \underbrace{\mathbb{E}_{(z_t, r_t) \sim \mathcal{D}} [(\hat{r}_\theta(z_t) - r_t)^2]}_{\text{reward reconstruction}} \\ & + \gamma \underbrace{\mathbb{E}_{z_t \sim \mathcal{D}} [\text{D}_{\text{KL}}(\pi_\theta(\cdot | z_t) \| \hat{P}_i(\cdot | z_t))]}_{\text{Markov regularization}}. \end{aligned} \quad (14)$$

The three terms encourage the RM to (i) imitate observed transition patterns, (ii) reconstruct the weak reward signal, and (iii) remain aligned with the empirical Markov structure of each image.

### 3.5. Self-Evolving Loop

**Overall Workflow.**

1. **Sampling Phase (Bandit):** UCB-driven exploration generates multiple weak Markov trajectories  $\mathcal{T}_i$  for each image  $x_i$ , while Dirichlet updates produce the corresponding transition prior  $\hat{P}_i$ . These image-level units  $(\mathcal{T}_i, \hat{P}_i)$  are accumulated into the offline buffer  $\mathcal{D}$ .
2. **Offline Training:** The Reward–Policy Model (RM) is optimized on  $\mathcal{D}$  by minimizing  $\mathcal{L}_{\text{RM}}$ , recovering both transition behavior and weak reward patterns.
3. **Inference Phase:** During deployment, UCB exploration is replaced by RM predictions, enabling the agent to perform self-evolving reasoning without online sampling.

**Inference Decision Rules.** During deployment, the next weak Markov unit is selected as

$$z_{t+1} = \begin{cases} \arg \max_z \pi_\theta(z | z_t) \\ \arg \max_z \hat{r}_\theta(z) \\ \arg \max_z [\alpha \log \pi_\theta(z | z_t) \\ + (1 - \alpha) \widehat{\text{norm}}(\hat{r}_\theta(z))], \end{cases} \quad (15)$$

*Selection modes:* (i) policy-driven (default); (ii) reward-driven; (iii) hybrid, where  $\alpha \in [0, 1]$  balances the two heads.

**Complexity and Practicality.** The sampling cost scales linearly with trajectory length and action space size. The RM is a compact 3-layer MLP with dual heads (20MB), keeping OVOD-Agent **LLM-free** and introducing only minor memory overhead during inference, allowing it to be incorporated into different OVOD detectors with minimal modification.

## 4. Experiments

In this section, we evaluate the performance of **OVOD-Agent** on the COCO [23] and LVIS [13] benchmarks, conduct ablation studies to analyze its core components, and discuss limitations as well as representative failure cases.

### 4.1. Main results

We evaluate **OVOD-Agent** on the **COCO** and **LVIS** benchmarks under the open-vocabulary object detection (OVOD) setting by plugging it into three representative base detectors: **GroundingDINO**, **YOLO-World**, and **DetCLIP**. The overall results are summarized in Table 2.

**Datasets.** Open-vocabulary detectors typically struggle on *rare categories*, which are heavily underrepresented in existing training corpora. To evaluate both general and long-tailed performance, we adopt the COCO and LVIS benchmarks under the standard open-vocabulary detection setting. For LVIS, we report results on the full LVIS val split (20k images) and the widely used LVIS minival subset (5k images). Following prior works such as Detic [43] and GLIP [21], LVIS minival is formed by selecting the first 5k images in the official validation index, providing a fast yet comparable protocol for OVD evaluation.

**Results analysis.** As shown in Table 2, **OVOD-Agent** provides moderate and consistent improvements across all base detectors. On LVIS val, the rare-category metric  $\text{AP}_r$  improves by **+2.7**, **+2.4**, and **+1.6** for GroundingDINO, YOLO-World, and DetCLIP, respectively, demonstrating the agent’s effectiveness in long-tailed recognition. These improvements remain consistent on the LVIS minival subset, where OVOD-Agent increases  $\text{AP}_r$  by **+1.6**, **+1.8**, and **+1.4**. In all cases, the gains in overall AP are small (within **+0.3–0.7**), indicating that the method enhances rare categories without negatively affecting common or frequent ones. On COCO2017 val, where categories are more balanced, OVOD-Agent yields mild improvements of **+0.3–0.5** mAP, suggesting that the enhanced reasoning mechanism provides limited but stable benefits even for well-represented classes. Beyond accuracy, Table 2 also reports  $\Delta\text{Latency}$ , which measures the average per-image increase in inference time when the agent is integrated. Since each reasoning step adds one additional detector forward pass, the overhead grows approximately linearly with the trajectory length. This extra cost remains within an acceptable range while delivering consistent gains in rare-category accuracy, reflecting a favorable accuracy–efficiency trade-off.

### 4.2. Ablation Study

We conduct a series of ablation experiments to analyze the internal mechanisms of **OVOD-Agent**. All ablations are conducted on the **LVIS minival** using **GroundingDINO** as the representative base detector unless otherwise specified. Additional results on **YOLO-World** and **DetCLIPv3** are provided in the supplementary material to verify consistency across detectors. The ablation design aligns with the overall pipeline of OVOD-Agent and reflects its three-stage process: (1) the *sampling mechanism*, examining the efficiency of the UCB-based exploration strategy; (2) the *learning mechanism*, analyzing the effect of explicit Markov-state (Markov–Bandit) modeling in reward optimization; and (3) the *reasoning mechanism*, evaluating the contribution of Visual-CoT actions and visual priors. This organization mirrors the agent’s operational flow, providing a systematic validation of each component’s role and contribution.

#### 4.2.1. Effect of UCB Exploration

We compare the proposed UCB-based exploration policy with three standard baselines—Random, Greedy-Q, and  $\epsilon$ -Greedy ( $\epsilon=0.1$ ) under a unified weak-MDP formulation. All methods follow the same *convergence-based stopping criteria* defined in Sec. 3.3, ensuring fair comparison with equal termination conditions for both trajectory- and image-level processes.

**Evaluation metrics.** To assess exploration quality, we report two quantitative indicators: (i) **Top-K@Stop**, the mean

Table 2. **Main results on LVIS and COCO benchmarks.** OVOD-Agent improves rare-category detection ( $AP_r$ ) while maintaining stable overall accuracy (AP), with only a small increase in inference latency.

| Method             | LVIS <sup>val</sup> |        |        |            |               |             | LVIS <sup>minival</sup> |        |        |               | COCO <sup>2017val</sup> |      | $\Delta$ Latency (ms) |
|--------------------|---------------------|--------|--------|------------|---------------|-------------|-------------------------|--------|--------|---------------|-------------------------|------|-----------------------|
|                    | $AP_r$              | $AP_c$ | $AP_f$ | $AP_{all}$ | $\Delta AP_r$ | $\Delta AP$ | $AP_r$                  | $AP_c$ | $AP_f$ | $\Delta AP_r$ | $AP_{all}$              | mAP  |                       |
| GroundingDINO [25] | 30.2                | 47.8   | 53.2   | 43.7       | –             | –           | 35.4                    | 51.3   | 55.7   | –             | 52.1                    | 52.8 | –                     |
| + OVOD-Agent       | 32.9                | 48.5   | 53.6   | 44.4       | <b>+2.7</b>   | <b>+0.7</b> | 37.0                    | 52.1   | 56.3   | <b>+1.6</b>   | 52.7                    | 54.1 | <b>+120</b>           |
| YOLO-World [4]     | 22.8                | 32.3   | 36.2   | 33.3       | –             | –           | 27.6                    | 34.1   | 38.0   | –             | 35.4                    | 45.0 | –                     |
| + OVOD-Agent       | 25.2                | 33.0   | 36.5   | 33.8       | <b>+2.4</b>   | <b>+0.5</b> | 29.4                    | 35.0   | 38.2   | <b>+1.8</b>   | 35.9                    | 45.9 | <b>+90</b>            |
| DetCLIPv3 [40]     | 37.2                | 37.5   | 41.2   | 38.9       | –             | –           | 45.1                    | 47.7   | 46.7   | –             | 47.0                    | 49.0 | –                     |
| + OVOD-Agent       | 38.8                | 38.3   | 41.4   | 39.3       | <b>+1.6</b>   | <b>+0.4</b> | 46.5                    | 48.4   | 46.8   | <b>+1.4</b>   | 47.5                    | 49.8 | <b>+100</b>           |

reward of the top  $K = \lfloor 0.1n_x \rfloor$  trajectories (with  $n_x$  denoting the number of sampled trajectories for image  $x$ ) before convergence, which reflects the quality of high-reward trajectories discovered by the policy; (ii) **Pareto-Win Rate (PWR)**, the percentage of images where a policy achieves higher Top-K with an equal or smaller sampling budget, reflecting exploration efficiency. Higher values indicate stronger exploration. and (iii) **AI/Human Score**, where GPT-5 [27] and human annotators jointly evaluate trajectory coherence to capture both model-based consistency and human-perceived reasoning quality.

Table 3. Comparison of exploration strategies under the unified stopping protocol. Higher is better for all metrics.

| Strategy           | Top-K@Stop       | PWR(%)      | AI             | Human          |
|--------------------|------------------|-------------|----------------|----------------|
| Random             | 0.54±0.02        | 19.1        | 2.8±0.2        | 2.7±0.3        |
| Greedy-Q           | 0.59±0.02        | 29.7        | 3.2±0.2        | 3.1±0.3        |
| $\epsilon$ -Greedy | 0.62±0.01        | 36.5        | 3.5±0.1        | 3.3±0.2        |
| <b>UCB (Ours)</b>  | <b>0.66±0.01</b> | <b>44.8</b> | <b>4.7±0.1</b> | <b>4.5±0.2</b> |

According to Table 3, the UCB policy achieves the highest Top-K@Stop (**0.66**) and PWR (**44.8%**), consistently discovering more high-reward trajectories under the same stopping criteria. It also obtains higher AI and Human evaluation scores (4.7 and 4.5), indicating that the sampled trajectories exhibit clearer semantic progression and are judged as more coherent and meaningful. These advantages arise purely from improved exploration behavior rather than increased sampling.

#### 4.2.2. Impact of Markov-State Modeling in RM Training

We compare two reward model (RM) optimization schemes: (1) a *trajectory-only* baseline trained purely from sequential samples, and (2) the full *Markov-Bandit* variant that explicitly incorporates the empirical transition matrix  $\hat{P}(a'|a, x)$  together with a KL-based transition regularization. This design enforces transition-consistent updates, mitigating unstable reward propagation and overfitting to local action modes.

All models are evaluated using four metrics: RM loss stability, action entropy, and downstream detection accuracy (AP and  $AP_r$ ). Action entropy reflects the diversity and uncertainty of the learned policy—higher entropy indicates richer exploration, while lower values suggest overconfident or mode-collapsed behavior.

Table 4. Ablation on explicit Markov-state modeling in reward optimization. Metrics include RM loss stability, action entropy, and detection performance (AP and  $AP_r$ ) measured on the LVIS<sup>minival</sup> benchmark.

| Training Scheme      | RM Loss Std  | Action Entropy | AP          | $AP_r$      |
|----------------------|--------------|----------------|-------------|-------------|
| Trajectory-only      | 0.037        | 1.41           | 38.2        | 19.0        |
| <b>Markov-Bandit</b> | <b>0.028</b> | <b>1.55</b>    | <b>39.4</b> | <b>20.3</b> |

Results in Table 4 show that the Markov-Bandit variant reduces RM loss variance from **0.037** to **0.028**, indicating more stable reward training. It also increases action entropy (1.41  $\rightarrow$  **1.55**), suggesting more balanced exploration. These improvements translate into consistent downstream gains on LVIS minival, with AP rising from 38.2  $\rightarrow$  **39.4** and  $AP_r$  from 19.0  $\rightarrow$  **20.3**. These gains account for part of the overall improvement observed in the full OVOD-Agent, which additionally incorporates UCB exploration and Visual-CoT reasoning. This demonstrates that explicit Markov-state modeling acts as an effective structural regularizer that stabilizes reward learning and contributes meaningfully to final detection performance.

#### 4.2.3. Contribution of Visual-CoT Actions and Priors

We progressively expand the agent’s action space from a single textual reasoning operation ( $a_1$ ) to the full Visual-CoT action set ( $a_1$ – $a_7$ ), which incorporates attribute- and geometry-aware cues such as color, texture, material, lighting, and spatial priors. All experiments are conducted on the LVIS minival split using GroundingDINO as the base detector.

As shown in Table 5, attribute-level Visual-CoT actions lead to consistent performance gains. Introducing only the dictionary-based textual action ( $+a_1$ ) yields a moderate im-

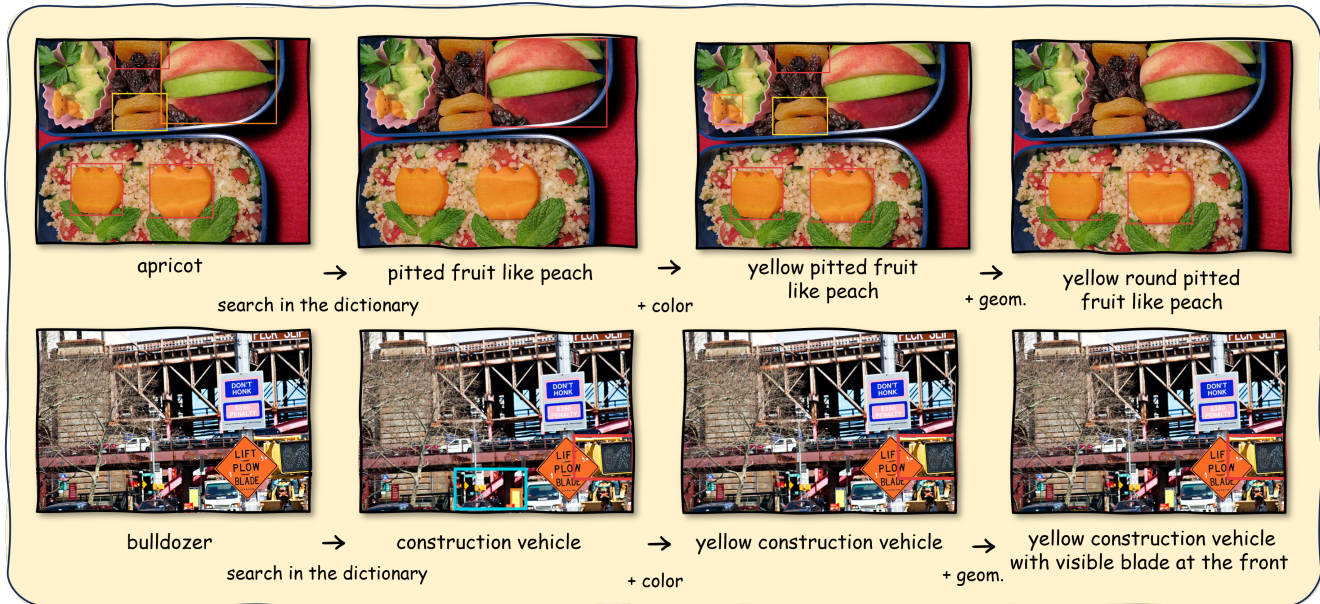


Figure 3. **Failure cases of OVOD-Agent.** Representative examples where the agent fails to correctly identify rare or occluded objects.

Table 5. Ablation on Visual-CoT actions and visual priors. Metrics are evaluated on the LVIS minival dataset.

| Action Set                                | $AP_r$      | $AP_c$      | $AP_f$      | AP          |
|---|-------------|-------------|-------------|-------------|
| Baseline                                  | 35.4        | 51.3        | 55.7        | 52.2        |
| + $a_1$                                   | 36.5        | 52.1        | 55.9        | 53.6        |
| <b>+<math>a_1</math>-<math>a_7</math></b> | <b>38.1</b> | <b>52.8</b> | <b>56.3</b> | <b>54.5</b> |

provement, raising  $AP_r$  from 35.4 to 36.5. When the full action space (+ $a_1$ - $a_7$ ) is enabled, rare-category performance further increases to **38.1**  $AP_r$ , accompanied by similar gains in  $AP_c$ ,  $AP_f$ , and overall AP. These results demonstrate that structured Visual-CoT actions provide richer semantic refinements and more discriminative attribute cues, thereby enhancing open-vocabulary generalization.

### 4.3. Limitations and Failure Analysis

While **OVOD-Agent** improves rare-category detection and provides interpretable reasoning traces, several limitations remain in challenging long-tail scenarios. Figure 3 illustrates two representative failure modes.

**Visual-Semantic Degradation.** In the first example, the target class is *apricot*, but the image actually shows a dried fruit slice whose appearance strongly deviates from the canonical visual prior encoded in the detector. Such mismatch causes the reasoning process to reinforce idealized attributes from language priors rather than adapt to degraded visual cues. Since “dried” or otherwise non-canonical object states appear rarely in training data, the

corresponding transition statistics become sparse, making reward updates unstable.

**Tiny Object and Cluttered Context.** The second example involves a *bulldozer* that is small, partially occluded, and embedded in a visually cluttered environment. In this setting, geometric ( $a_5$ ) and spatial ( $a_7$ ) actions provide weak or noisy reward signals, leading the policy to repeatedly fall back to dictionary lookups ( $a_1$ ) without improving localization. Strong background clutter can also produce misleadingly high CLIP similarities with related categories such as *truck* or *sign*, confusing the reward model. Sparse transition observations for rare classes exacerbate these effects.

**Discussion.** These cases reveal two key limitations of OVOD-Agent: (1) sensitivity to semantic-visual mismatch when object appearance shifts away from canonical forms, and (2) difficulty handling tiny or heavily occluded rare objects in cluttered contexts. Addressing these challenges may require stronger visual priors or adaptive reasoning strategies for out-of-distribution scenarios.

## 5. Conclusions

We present OVOD-Agent, a lightweight Markov-Bandit framework that transforms open-vocabulary detection from static matching into proactive visual reasoning. By grounding its Visual-CoT in a discrete, weakly Markovian state distribution, combined with uncertainty-aware exploration, the agent consistently improves performance across diverse backbones, especially on rare categories. It provides a scalable foundation for self-evolving visual reasoning in open-world settings.

## References

- [1] Peter Auer, Nicolo Cesa-Bianchi, and Paul Fischer. Finite-time analysis of the multiarmed bandit problem. *Machine learning*, 47(2):235–256, 2002. 3
- [2] Lorenzo Bianchi, Fabio Carrara, Nicola Messina, Claudio Gennaro, and Fabrizio Falchi. The devil is in the fine-grained details: Evaluating open-vocabulary object detectors for fine-grained understanding. In *Proceedings of the IEEE/CVF Conference on Computer Vision and Pattern Recognition (CVPR)*, pages 22520–22529, 2024. 2
- [3] Lili Chen, Kevin Lu, Aravind Rajeswaran, Kimin Lee, Aditya Grover, Michael Laskin, Pieter Abbeel, Aravind Srinivas, and Igor Mordatch. Decision transformer: Reinforcement learning via sequence modeling, 2021. 3
- [4] Tianheng Cheng, Lin Song, Yixiao Ge, Wenyu Liu, Xinggang Wang, and Ying Shan. Yolo-world: Real-time open-vocabulary object detection. In *Proceedings of the IEEE/CVF conference on computer vision and pattern recognition*, pages 16901–16911, 2024. 1, 7
- [5] Hojun Choi, Youngsun Lim, Jaeyo Shin, and Hyunjung Shim. Cot-pl: Visual chain-of-thought reasoning meets pseudo-labeling for open-vocabulary object detection, 2025. 2
- [6] Paul F Christiano, Jan Leike, Tom Brown, Miljan Martic, Shane Legg, and Dario Amodei. Deep reinforcement learning from human preferences. *Advances in neural information processing systems*, 30, 2017. 3
- [7] Emanuele Crisostomi, Robert Shorten, Sonja Stüdl, and Fabian Wirth. *Electric and plug-in hybrid vehicle networks: optimization and control*. CRC Press, 2017. 2
- [8] Yu Du, Fangyun Wei, Ziheng Zhang, Miaojing Shi, Yue Gao, and Guoqi Li. Learning to prompt for open-vocabulary object detection with vision-language model, 2022. 1
- [9] Zane Durante, Qiuyuan Huang, Naoki Wake, Ran Gong, Jae Sung Park, Bidipta Sarkar, Rohan Taori, Yusuke Noda, Demetri Terzopoulos, Yejin Choi, Katsushi Ikeuchi, Hoi Vo, Li Fei-Fei, and Jianfeng Gao. Agent ai: Surveying the horizons of multimodal interaction, 2024. 2
- [10] Yunfan Gao, Yun Xiong, Xinyu Gao, Kangxiang Jia, Jinliu Pan, Yuxi Bi, Yi Dai, Jiawei Sun, Meng Wang, and Haofen Wang. Retrieval-augmented generation for large language models: A survey, 2024. 2
- [11] Yunhao Ge, Jie Ren, Andrew Gallagher, Yuxiao Wang, Ming-Hsuan Yang, Hartwig Adam, Laurent Itti, Balaji Lakshminarayanan, and Jiaping Zhao. Improving zero-shot generalization and robustness of multi-modal models. In *Proceedings of the IEEE/CVF Conference on Computer Vision and Pattern Recognition (CVPR)*, pages 11093–11101, 2023. 1
- [12] Xiuye Gu, Tsung-Yi Lin, Weicheng Kuo, and Yin Cui. Open-vocabulary object detection via vision and language knowledge distillation. *arXiv preprint arXiv:2104.13921*, 2021. 1
- [13] Agrim Gupta, Piotr Dollar, and Ross Girshick. Lvis: A dataset for large vocabulary instance segmentation. In *Proceedings of the IEEE/CVF Conference on Computer Vision and Pattern Recognition (CVPR)*, 2019. 6
- [14] Danijar Hafner, Timothy Lillicrap, Mohammad Norouzi, and Jimmy Ba. Mastering atari with discrete world models, 2022. 3
- [15] Jonathan Ho, Ajay Jain, and Pieter Abbeel. Denoising diffusion probabilistic models, 2020. 2
- [16] Sheng Jin, Xueying Jiang, Jiaying Huang, Lewei Lu, and Shijian Lu. Llm meets vlms: Boost open vocabulary object detection with fine-grained descriptors, 2024. 2
- [17] Jooyeon Kim, Eulrang Cho, Sehyung Kim, and Hyunwoo J. Kim. Retrieval-augmented open-vocabulary object detection. In *Proceedings of the IEEE/CVF Conference on Computer Vision and Pattern Recognition (CVPR)*, pages 17427–17436, 2024. 2
- [18] Louis Y Kim, Michelle Karker, Victoria Valledor, Seiyoung C Lee, Karl F Brzozka, Margaret Duff, and Anthony Palladino. An iterative feedback mechanism for improving natural language class descriptions in open-vocabulary object detection. In *Automatic Target Recognition XXXV*, pages 57–69. SPIE, 2025. 2
- [19] John Langford and Tong Zhang. The epoch-greedy algorithm for multi-armed bandits with side information. *Advances in neural information processing systems*, 20, 2007. 3
- [20] Junnan Li, Dongxu Li, Silvio Savarese, and Steven Hoi. Blip-2: Bootstrapping language-image pre-training with frozen image encoders and large language models, 2023. 2
- [21] Liunian Harold Li, Pengchuan Zhang, Haotian Zhang, Jianwei Yang, Chunyuan Li, Yiwu Zhong, Lijuan Wang, Lu Yuan, Lei Zhang, Jenq-Neng Hwang, Kai-Wei Chang, and Jianfeng Gao. Grounded language-image pre-training. In *Proceedings of the IEEE/CVF Conference on Computer Vision and Pattern Recognition (CVPR)*, pages 10965–10975, 2022. 1, 6
- [22] Zejun Li, Ruipu Luo, Jiwen Zhang, Minghui Qiu, Xuanjing Huang, and Zhongyu Wei. VoCoT: Unleashing visually grounded multi-step reasoning in large multi-modal models. In *Proceedings of the 2025 Conference of the Nations of the Americas Chapter of the Association for Computational Linguistics: Human Language Technologies (Volume 1: Long Papers)*, pages 3769–3798, Albuquerque, New Mexico, 2025. Association for Computational Linguistics. 2
- [23] Tsung-Yi Lin, Michael Maire, Serge Belongie, James Hays, Pietro Perona, Deva Ramanan, Piotr Dollár, and C Lawrence Zitnick. Microsoft coco: Common objects in context. In *European conference on computer vision*, pages 740–755. Springer, 2014. 6
- [24] Haotian Liu, Chunyuan Li, Qingyang Wu, and Yong Jae Lee. Visual instruction tuning, 2023. 2
- [25] Shilong Liu, Zhaoyang Zeng, Tianhe Ren, Feng Li, Hao Zhang, Jie Yang, Qing Jiang, Chunyuan Li, Jianwei Yang, Hang Su, et al. Grounding dino: Marrying dino with grounded pre-training for open-set object detection. In *European conference on computer vision*, pages 38–55. Springer, 2024. 1, 7, 2
- [26] Furkan Mumcu, Michael J. Jones, Anoop Cherian, and Yasin Yilmaz. Llm-guided agentic object detection for open-world understanding, 2025. 2

- [27] OpenAI. Openai gpt-5 model release. <https://openai.com/index/introducing-gpt-5/>, 2025. Accessed: 2025-08-07. 7
- [28] Long Ouyang, Jeffrey Wu, Xu Jiang, Diogo Almeida, Carroll Wainwright, Pamela Mishkin, Chong Zhang, Sandhini Agarwal, Katarina Slama, Alex Ray, et al. Training language models to follow instructions with human feedback. *Advances in neural information processing systems*, 35:27730–27744, 2022. 3
- [29] Sarah Parisot, Yongxin Yang, and Steven McDonagh. Learning to name classes for vision and language models. In *Proceedings of the IEEE/CVF Conference on Computer Vision and Pattern Recognition (CVPR)*, pages 23477–23486, 2023. 1
- [30] Zhiliang Peng, Wenhui Wang, Li Dong, Yaru Hao, Shaohan Huang, Shuming Ma, and Furu Wei. Kosmos-2: Grounding multimodal large language models to the world, 2023. 2
- [31] Sarah Pratt, Ian Covert, Rosanne Liu, and Ali Farhadi. What does a platypus look like? generating customized prompts for zero-shot image classification. In *Proceedings of the IEEE/CVF International Conference on Computer Vision (ICCV)*, pages 15691–15701, 2023. 1
- [32] Alec Radford, Jong Wook Kim, Chris Hallacy, Aditya Ramesh, Gabriel Goh, Sandhini Agarwal, Girish Sastry, Amanda Askell, Pamela Mishkin, Jack Clark, Gretchen Krueger, and Ilya Sutskever. Learning transferable visual models from natural language supervision, 2021. 1
- [33] Yongming Rao, Wenliang Zhao, Guangyi Chen, Yansong Tang, Zheng Zhu, Guan Huang, Jie Zhou, and Jiwen Lu. Denseclip: Language-guided dense prediction with context-aware prompting, 2022. 2
- [34] Timo Schick, Jane Dwivedi-Yu, Roberto Dessi, Roberta Raileanu, Maria Lomeli, Eric Hambro, Luke Zettlemoyer, Nicola Cancedda, and Thomas Scialom. Toolformer: Language models can teach themselves to use tools. In *Advances in Neural Information Processing Systems*, pages 68539–68551. Curran Associates, Inc., 2023. 2
- [35] Hao Shao, Shengju Qian, Han Xiao, Guanglu Song, Zhuofan Zong, Letian Wang, Yu Liu, and Hongsheng Li. Visual cot: Advancing multi-modal language models with a comprehensive dataset and benchmark for chain-of-thought reasoning, 2024. 2
- [36] Jason Wei, Xuezhi Wang, Dale Schuurmans, Maarten Bosma, brian ichter, Fei Xia, Ed Chi, Quoc V Le, and Denny Zhou. Chain-of-thought prompting elicits reasoning in large language models. In *Advances in Neural Information Processing Systems*, pages 24824–24837. Curran Associates, Inc., 2022. 2
- [37] Wen Yang, Minpeng Liao, and Kai Fan. Markov chain of thought for efficient mathematical reasoning, 2025. 2
- [38] Lewei Yao, Jianhua Han, Youpeng Wen, Xiaodan Liang, Dan Xu, Wei Zhang, Zhenguo Li, Chunjing Xu, and Hang Xu. Detclip: Dictionary-enriched visual-concept paralleled pre-training for open-world detection, 2022. 1
- [39] Lewei Yao, Jianhua Han, Xiaodan Liang, Dan Xu, Wei Zhang, Zhenguo Li, and Hang Xu. Detclipv2: Scalable open-vocabulary object detection pre-training via word-region alignment, 2023.
- [40] Lewei Yao, Renjie Pi, Jianhua Han, Xiaodan Liang, Hang Xu, Wei Zhang, Zhenguo Li, and Dan Xu. Detclipv3: Towards versatile generative open-vocabulary object detection. In *Proceedings of the IEEE/CVF conference on computer vision and pattern recognition*, pages 27391–27401, 2024. 1, 7
- [41] Shunyu Yao, Jeffrey Zhao, Dian Yu, Nan Du, Izhak Shafran, Karthik R. Narasimhan, and Yuan Cao. ReAct: Synergizing Reasoning and Acting in Language Models. In *Proceedings of the Eleventh International Conference on Learning Representations (ICLR 2023)*, Kigali, Rwanda, 2023. ICLR. 2
- [42] Yiwu Zhong, Jianwei Yang, Pengchuan Zhang, Chunyuan Li, Noel Codella, Liunian Harold Li, Luowei Zhou, Xiyang Dai, Lu Yuan, Yin Li, and Jianfeng Gao. Regionclip: Region-based language-image pretraining. In *Proceedings of the IEEE/CVF Conference on Computer Vision and Pattern Recognition (CVPR)*, pages 16793–16803, 2022. 2
- [43] Xingyi Zhou, Rohit Girdhar, Armand Joulin, Philipp Krähenbühl, and Ishan Misra. Detecting twenty-thousand classes using image-level supervision. In *European conference on computer vision*, pages 350–368. Springer, 2022. 1, 6
- [44] Xingyi Zhou, Rohit Girdhar, Armand Joulin, Philipp Krähenbühl, and Ishan Misra. Detecting twenty-thousand classes using image-level supervision. In *European conference on computer vision*, pages 350–368. Springer, 2022. 1
- [45] Deyao Zhu, Jun Chen, Xiaoqian Shen, Xiang Li, and Mohamed Elhoseiny. Minigpt-4: Enhancing vision-language understanding with advanced large language models, 2023. 2

# OVOD-Agent: A Markov-Bandit Framework for Proactive Visual Reasoning and Self-Evolving Detection

## Supplementary Material

### 6. Appendix

This appendix provides additional technical details that complement the main paper. We first present the full set of visual-action operators used by **OVOD-Agent**. Next, we provide an expanded case study that demonstrates how the agent incrementally refines its textual hypotheses using both low-level and high-level visual cues. We further include a comparison between OVOD-Agent and other LLM-based COT methods, emphasizing the differences in inference latency across these approaches. Finally, we provide the exact GPT-5 evaluation prompts and scoring rubric used to assess trajectory coherence and groundedness, ensuring transparency and reproducibility of our analysis.

### 6.1. Visual Actions Space

This section presents the pseudocode for the seven interpretable visual actions ( $a_1$ – $a_7$ ) used by **OVOD-Agent**, as summarized in Algorithm 2. Each action extracts a specific visual cue from the ROI (e.g. color, texture, geometry, background, lighting, or spatial relation) and maps it to a short linguistic attribute that is later used to update the evolving caption in the main reasoning algorithm.

To ensure reproducibility, all visual cues are computed using standard computer vision toolkits. Specifically, we employ **OpenCV** for RGB–HSV color conversion, K-means clustering, edge detection, and basic shape analysis; **scikit-image** for LBP/GLCM texture extraction, brightness

---

**Algorithm 2:** Visual Actions  $a_1$ – $a_7$

---

```
1 Function  $a_1$ : Dictionary:
2   obj  $\leftarrow$  PARSE_NOUN(c)
3   syn  $\leftarrow$  WORDNET_SYN(obj)
4   hyp  $\leftarrow$  WORDNET_HYPER(obj)
5   cand  $\leftarrow$  syn  $\cup$  hyp
6   tokens  $\leftarrow$  FILTER_VISUAL_TERMS(cand)
7   phrase  $\leftarrow$  FORMAT("a object", tokens)
8 end
9 Function  $a_2$ : Color:
10  hsv  $\leftarrow$  TO_HSV(r)
11  clst  $\leftarrow$  KMEANS(hsv, 3)
12  dom  $\leftarrow$  LARGEST_CLUSTER(clst)
13  col  $\leftarrow$  HSV_TO_COLOR(dom)
14  phrase  $\leftarrow$  FORMAT("color", col)
15 end
16 Function  $a_3$ : Texture:
17  lbp  $\leftarrow$  LBP(r)
18  glcm  $\leftarrow$  GLCM(r)
19  feats  $\leftarrow$  {lbp, glcm}
20  tex  $\leftarrow$  MATCH_TEXTURE(feats)
21  phrase  $\leftarrow$  FORMAT("texture", tex)
22 end
23 Function  $a_4$ : Background:
24  fg  $\leftarrow$  FG_MASK(r)
25  bg  $\leftarrow$  r - fg
26  clt  $\leftarrow$  BG_CLUTTER(bg)
27  tag  $\leftarrow$  IF(clt  $\dot{>}$   $\tau$ , "cluttered", "clean background")
28  phrase  $\leftarrow$  FORMAT("object against ", tag)
29 end
30 Function  $a_5$ : Geometry:
31  ar  $\leftarrow$  ASPECT_RATIO(r)
32  sc  $\leftarrow$  BBOX_SCALE(r)
33  geom  $\leftarrow$  CLASSIFY_GEOM(ar, sc)
34  phrase  $\leftarrow$  FORMAT("shaped", geom)
35 end
36 Function  $a_6$ : Lighting:
37  hist  $\leftarrow$  V_CHANNEL_HIST(r)
38  mean  $\leftarrow$  MEAN(hist)
39  var  $\leftarrow$  VAR(hist)
40  cond  $\leftarrow$  IF3( mean  $<$   $\tau_{\text{dark}}$ , "underexposed",
41                mean  $>$   $\tau_{\text{bright}}$ , "overexposed",
42                var  $>$   $\tau_{\text{shadow}}$ , "shadowed",
43                "well-lit" )
44  phrase  $\leftarrow$  FORMAT("lighting", cond)
45 end
46 Function  $a_7$ : Spatial:
47  rel  $\leftarrow$  SPATIAL_REL(r, layout)
48  phrase  $\leftarrow$  FORMAT("the object", rel)
49 end
```

---

Table 6. **Comparison with LLM-guided reasoning modules (all methods use GroundingDINO-B as the base detector).** OVOD-Agent achieves competitive rare-category improvements while keeping inference in the *millisecond* regime, whereas LLM-based CoT methods require *second-level* latency.

| Method                                       | LVIS AP <sub>r</sub> | AP <sub>c</sub> | AP <sub>f</sub> | AP <sub>all</sub> | COCO AP <sub>50</sub> <sup>N</sup> | Avg Latency  | Worst-case    | LLM Calls |
|--|----------------------|-----------------|-----------------|-------------------|------------------------------------|--------------|---------------|-----------|
| GroundingDINO (baseline) [25]                | 35.4                 | 51.3            | 55.7            | 52.1              | 30.8                               | 25 ms        | 25 ms         | 0         |
| RALF (LLM-based RAG) [17]                    | 38.6                 | 52.0            | 56.1            | 52.9              | 33.2                               | 1.5 s        | 3.0 s         | 3–7       |
| CoT-PL (LLM prompt reasoning) [5]            | 37.4                 | 51.8            | 55.9            | 52.7              | 32.5                               | 1.2 s        | 2.5 s         | 2–5       |
| DVDet (offline VQA-refined descriptors) [16] | 36.2                 | 51.0            | 55.3            | 52.0              | 31.4                               | 30 ms        | 45 ms         | 0         |
| OVOD-Agent (Ours)                            | <b>37.0</b>          | <b>52.1</b>     | <b>56.3</b>     | <b>52.7</b>       | <b>33.4</b>                        | <b>55 ms</b> | <b>175 ms</b> | <b>0</b>  |

histogram estimation, and foreground/background masking; and NumPy/SciPy for region-level statistics, histogram aggregation, and geometric feature computation.

These operations enable OVOD-Agent to extract stable and interpretable visual cues directly from the image, providing a consistent basis for subsequent textual refinement.

## 6.2. Detailed Step-by-Step Case Study

To illustrate how **OVOD-Agent** performs multi-step visual reasoning, we present a detailed case study (Fig. 4) that traces the complete prediction trajectory from an initial noun-only caption to a fully grounded, attribute-rich description. At each reasoning step, the agent executes one visual action, extracts a specific cue from the ROI (e.g. color via HSV analysis, texture via LBP/GLCM, or high-level cues from container/background geometry), converts the cue into a linguistic attribute, and updates the slot-based caption accordingly. For each step, we report: (1) the extracted visual evidence, (2) the updated caption, (3) the reward produced by the RM, and (4) the detector’s grounding response (score and IoU). This case study demonstrates how progressive, attribute-aware refinement enables **OVOD-Agent** to stabilize open-vocabulary grounding even when initial predictions are incomplete or the detector temporarily fails to produce a bounding box.

## 6.3. Comparison with LLM-based CoT Methods

To contextualize different refinement paradigms, this supplementary section provides additional comparisons between OVOD-Agent and several representative LLM-guided reasoning modules, including RALF (LLM-based RAG), CoT-PL (LLM-prompted refinement), and DVDet (offline VQA-based descriptor enhancement). LLM-driven CoT approaches typically rely on a cyclic pipeline of “detection → LLM rewriting → re-detection”, where each iteration requires a separate LLM call. As a result, their overall latency is dominated by LLM response time, often reaching the 1–3 second range.

DVDet does not invoke LLMs during inference and therefore runs at a speed close to the underlying detector. However, it still depends on large VQA models during training to generate or refine fine-grained textual descriptors, which incurs non-trivial additional computational and time

costs.

In contrast, OVOD-Agent adopts a completely different strategy: all refinement operations are performed through lightweight visual actions (color, texture, geometry, background, spatial cues), each requiring only a single forward pass of GroundingDINO. With an average of roughly 2.2 steps, the end-to-end latency remains firmly in the millisecond regime (55 ms).

Table 6 summarizes these results. LLM-driven CoT methods provide noticeable rare-category improvements but suffer from substantial latency; DVDet avoids online LLM calls at inference time but carries a higher offline training cost; and OVOD-Agent achieves the best accuracy–cost balance, offering competitive gains with minimal additional overhead.

## 6.4. GPT-5 Trajectory Scoring

For completeness, we include the prompt template used to query GPT-5 as an offline evaluator. GPT-5 does not participate in inference; it is used only to assign a continuous weak score to each sampled trajectory. As shown in Fig. 5, the evaluation protocol consists of an instruction prompt (defining GPT-5’s role and evaluation objective) and an input prompt containing the trajectory details. GPT-5 rates each trajectory according to the four criteria introduced in the main paper, and outputs a final aggregated score in the range [0, 5] in JSON format.

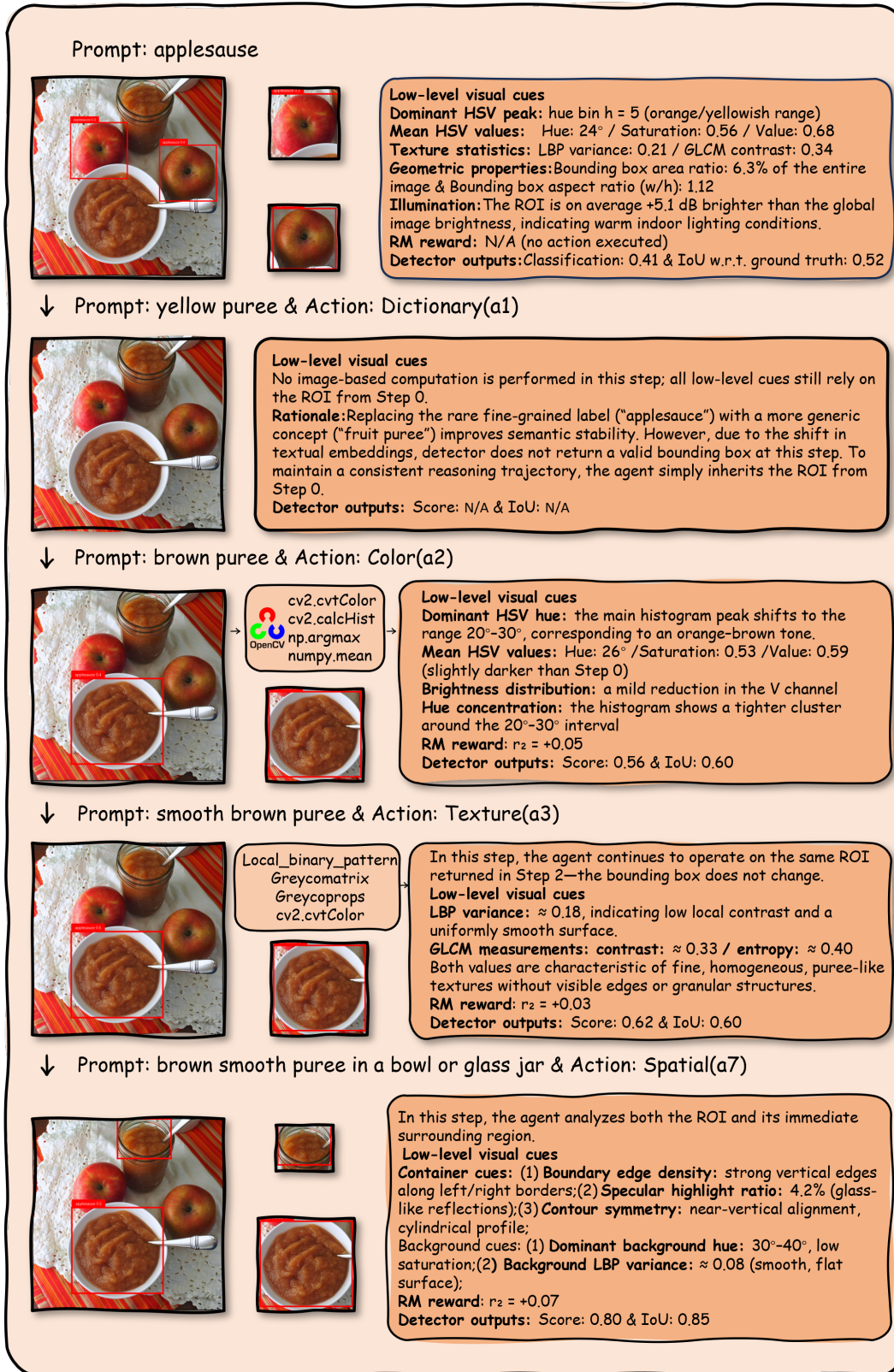


Figure 4. Step-by-step Case Study of **OVOD-Agent**, showing how visual actions (color, texture, container, background, spatial cues) progressively refine the caption and stabilize detector grounding.

**---Role---**

You are an expert evaluator specializing in multimodal reasoning and open-vocabulary visual grounding. Your responsibility is to assess the quality of visual reasoning trajectories generated by different sampling strategies.

**---Goal---**

You will rate a single trajectory sampled from one of four strategies (Random, Greedy-Q,  $\epsilon$ -Greedy, UCB). Evaluate the trajectory using four criteria:

- **Trajectory Consistency:** Whether the sequence of actions forms a stable and contradiction-free reasoning process.
- **Visual Groundedness:** Whether inferred attributes (color, texture, geometry, spatial cues) match the ROI appearance.
- **Informational Gain:** Whether each step adds clearer, more specific, and more discriminative detail to the caption.
- **Detector Synergy:** Whether caption updates improve or stabilize detector confidence (score, IoU).

For each trajectory, provide a continuous score for all four criteria following the rubric above, and then compute and output the final total score in the range [0, 5].

**Evaluation Instruction Prompt**

Here is the trajectory produced by a sampling strategy: **{StrategyName}**

Here are the trajectory details:

- **ROI description:** **{ROI\_Text}**
- **Executed actions:** **{Action\_List}**
- **Intermediate captions:** **{Caption\_List}**
- **Detector feedback (score, IoU):** **{Detector\_List}**

Evaluate this trajectory using the four criteria listed above and provide a continuous score for each criterion.

Output your evaluation in the following JSON format:

```
{
  "Trajectory_Consistency": { "Score": "<float in [0,2.0]>", "Explanation": "<reasoning>" },
  "Visual_Groundedness": { "Score": "<float in [0,1.5]>", "Explanation": "<reasoning>" },
  "Information_Gain": { "Score": "<float in [0,1.0]>", "Explanation": "<reasoning>" },
  "Detector_Synergy": { "Score": "<float in [0,0.5]>", "Explanation": "<reasoning>" },
  "Total_Score": "<float in [0,5]>"
}
```

**Evaluation Input Prompt**

Figure 5. Evaluation protocol for GPT-5 trajectory scoring, including the instruction prompt defining the evaluator’s role and the input prompt containing the sampled trajectory.